2021 43rd Annual International Conference of the
IEEE Engineering in Medicine & Biology Society (EMBC)
Oct 31 - Nov 4, 2021. Virtual Conference

2021 43rd Annual International Conference of the IEEE Engineering in Medicine & Biology Society (EMBC) | 978-1-7281-1179-7/21/$31.00 ©2021 IEEE | DOI: 10.1109/EMBC46164.2021.9630016

Identification of COVID-19 Type Respiratory Disorders Using Channel State Analysis of Wireless Communications Links

Lana C. Lubecke, Khaldoon Ishmael, *Member,* Yao Zheng, *Member,* Olga Borić-Lubecke, *Fellow,* and Victor M. Lubecke, *Fellow, IEEE*

***Abstract*— One deadly aspect of COVID-19 is that those infected can often be contagious before exhibiting overt symptoms. While methods such as temperature checks and sinus swabs have aided with early detection, the former does not always provide a reliable indicator of COVID-19, and the latter is invasive and requires significant human and material resources to administer. This paper presents a non-invasive COVID-19 early screening system implementable with commercial off-the-shelf wireless communications devices. The system leverages the Doppler radar principle to monitor respiratory-related chest motion and identifies breathing rates that indicate COVID-19 infection. A prototype was developed from software-defined radios (SDRs) designed for 5G NR wireless communications and system performance was evaluated using a robotic mover simulating human breathing, and using actual breathing, resulting in a consistent respiratory rate accuracy better than one breath per minute, exceeding that used in common medical practice.**

***Clinical Relevance*—This establishes the potential efficacy of wireless communications based radar for recognizing respiratory disorders such as COVID-19.**

I. Introduction

COVID-19 symptoms on average start five to six days after exposure (incubation period) [1]. Generally, a person infected with COVID-19 is most contagious 1 to 2 days before experiencing symptoms [2], as illustrated in Fig. 1. The peak contagiousness during this period combined with virtually undetectable symptoms has contributed to the rapid spread of COVID-19. Recent research has found that an increase in respiratory rate is one of the earliest indicators of COVID-19, taking place before the more obvious symptoms set in. Normally, people take about 12 breaths per minute (0.2 Hz) with a peak to peak chest displacement of 1 cm [3]. People infected with COVID-19 typically exhibit breathing above 20 breaths per minute (0.5 Hz) [4-5]. One recent study showed that respiratory patterns derived from wrist-worn straps estimated respiratory rate based on heart rate can be used to detect COVID-19 before and during the early onset of other symptoms [6]. A radar-based method that directly measures respiration without wearing sensors in contact with the body would offer great potential for improving detection rates.

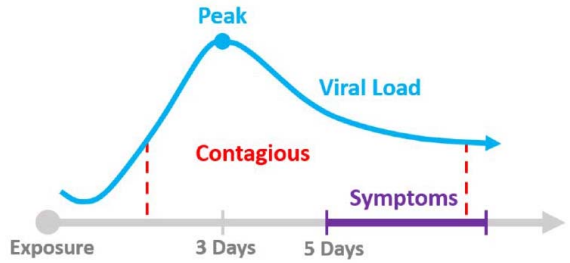

Fig.1. Timeline for COVID-19 infection.

The Doppler radar principle can be used to detect heart rate and breathing by measuring the phase shift resulting from respiratory body motion [7]. If two wireless communications devices are positioned such that their radio link bounces off a subject, the small fluctuations in the wireless channel state information (CSI) caused by body motion would contain the phase of the breathing pattern, as illustrated in Fig. 2. This principle has been used to measure respiration using wireless network interface cards (NICs) [8], which allow breathing detection at distances greater than 6 feet and remote operation that minimizes contagion exposure to the person administering the test. As the channel estimation process is common among various wireless communication protocols, the CSI data can be easily accessed to measure respiratory rate without modifications to the underlying hardware [8]. Thus, an effective method for assessing human respiration can be achieved using commonly available low-cost equipment that can be used to test many people in a wide range of circumstances. This includes leveraging systems that support

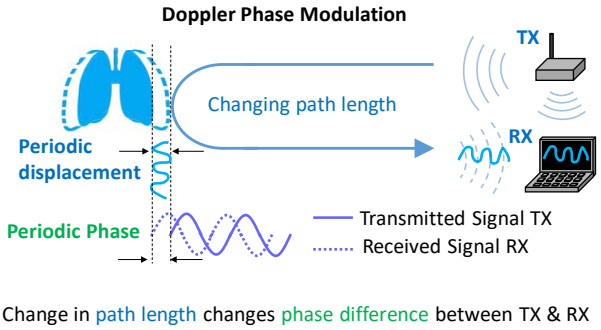

Fig. 2. Channel State Information (CSI) Doppler radar explanatory diagram. A transmitted signal, TX, is reflected from a breathing chest and shifts phase in proportion to the breathing motion. The received reflection, RX, is compared to TX, to output a displacement signal.

* This work was supported in part by the U.S. National Science Foundation under Grant IIS1915738. K. Ishmael is supported by a DoD SMART scholarship.

At the time of this work L. C. Lubecke was with Kalani High School, Honolulu, HI 96821 USA. She is currently with the California Institute of Technology, Pasadena, CA 91125 USA (e-mail: llubecke@caltech.edu).

K. Ishmael, Y. Zheng, Olga Borić-Lubecke, and Victor Lubecke are with the Electrical Engineering Department, University of Hawaii at Manoa, Honolulu, HI 96822 USA (phone: 760-900-6079; fax: 808-956-3427; e-mail: khaldoon@hawaii.edu).

wireless communications standards including Bluetooth, Wi-Fi, 4G LTE, and the emerging 5G NR (new radio) standard which can up-convert signals to millimeter wavelengths to support beamforming. Such systems would have the extreme advantage of allowing non-contact wireless sensing and health monitoring in many homes, workplaces, and public spaces without the need for introducing any new radar equipment.

II. Experimental Set-Up

The wireless-communications-based sensing system used was a customized 28 GHz OFDM 5G NR communication system, consisting of one pair of transmitter and receiver implemented with LabView and Ettus N210 Universal Software Radio Peripheral (USRP) with an output power of 15 dBm. The customized OFDM system had 32 pilot subcarriers and 128 data subcarriers, spanning half of the transmission bandwidth. The rest of the band was occupied by guard and cyclic prefix symbols. The bandwidth was set to 500 kHz during the experiment, resulting in 1.5626 kHz subcarrier spacing, 32 traces of accurate CSI measurements from pilot subcarriers separated by 7.8125 kHz intervals. The system was connected to a millimeter-wave beamforming development kit (BBox one/UD box from TMYTEK). The kit consisted of a 16-channel 24-31GHz phased array antenna, and a frequency up/down converter. The 3-dB beam aperture was 13 degrees horizontally and 14 degrees vertically. The angle coverage was +/-45 degrees horizontally and +/-60 degrees vertically.

The robotic mover consisted of a metallic target mechanically attached to a translation stage with one motion axis. The experimental setup is shown in Fig. 3. The target was a spherical shape with about a 5-cm diameter. The stage consisted of a via stepper drive mount controlled via a serial interface, which permitted automated movement sequences. The mount was a Griffin Motion LNS-100 Series Linear Stage with a Galil DMC30010. The position resolution, measured as commanded position vs. reported position, was typically within 1 µm. The robotic mover was moved sinusoidally at 10 different frequencies, and there were 2 trials per frequency. The robotic mover moved with an amplitude of 5 mm for all the trials. The frequencies tested were 0.2, 0.25, 0.3, 0.317, 0.333, 0.35, 0.367, 0.4, 0.45, and 0.5 Hz. The 6 middle frequencies are only 1 breath per minute apart. The signal was sampled at a rate of 10 samples per second, and the data were recorded for 120 seconds for each trial. The 5G NR cards were positioned at a distance of 2 meters from the robotic mover.

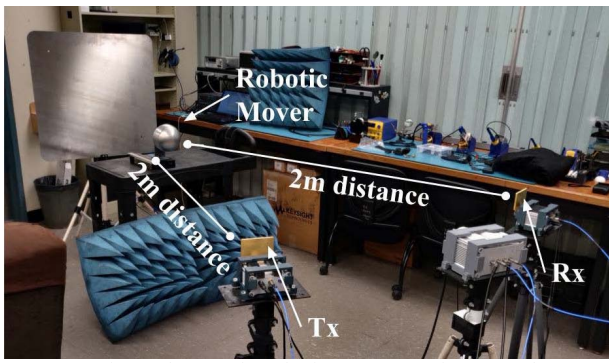

Fig. 3. Experimental set-up for robotic mover experiment. Both 5G NR wireless communications cards were 2 m away from the robotic mover.

III. Data Analysis

The CSI was recorded and analyzed for 32 channels, as shown in Fig. 4. Since phase shift caused by one breath spans

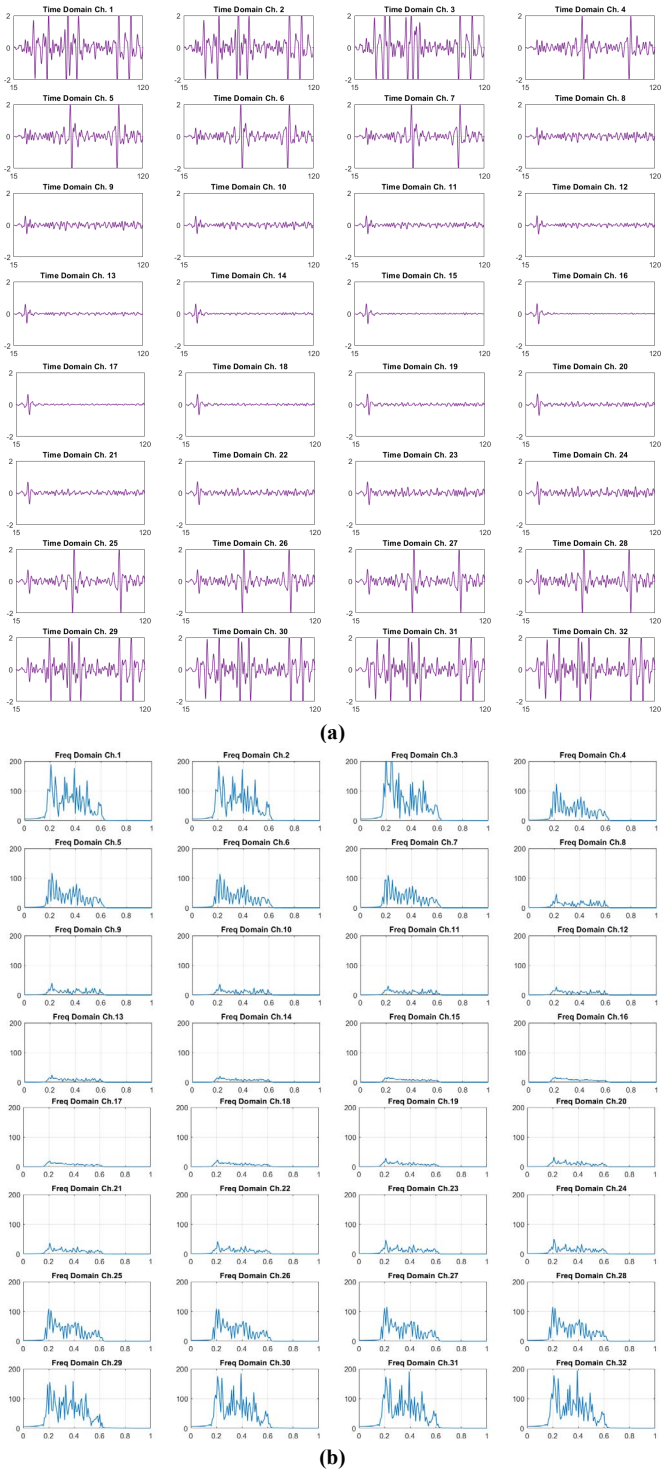

Fig. 4. Noise measured for all 32 channels plotted in time (a) and frequency (b) domains. Note channels 15, 16, and 17 are among those that contain significantly less noise.

multiple periods for the 28-GHz carrier signal, the phase angle was initially unwrapped. All channels were bandpass filtered between 0.195 and 0.6 Hz. However, it can be observed that there was still significant noise between 0.2 and 0.5 Hz that could not be filtered out since those frequencies are within the range of possible respiratory rates. In order to reduce noise, the individual channels of the wireless communications cards were examined with data from a trial where the mover was not moving, so that only noise was measured. Because each channel from the cards operates at a slightly different frequency, the frequency domain signals for each channel contained different magnitudes of noise, with some channels detecting very little noise. After examining noise levels in all 32 channels, it was concluded that channels 15, 16, and 17 recorded the least noise. After adjusting the algorithm to only operate on channels 15, 16, and 17, the algorithm was tested on the robotic mover data. The mode of the extracted frequencies was taken from the 3 channels with minimal noise because if one of the frequencies was different than the others, it was most likely because the algorithm identified a noise peak as the breathing frequency. In this case, the frequencies should not be averaged, but the most frequently occurring frequency should be regarded as the respiratory rate.

The algorithm used for recognizing rates indicative of COVID-19 goes as follows. First, the algorithm converts the signal from the time domain to the frequency domain by performing an FFT and then taking the absolute value. Then, a peak finder function is used to determine the frequency component with the highest peak. After the fundamental frequency is determined, the algorithm indicates that the respiratory rate is indicative of COVOD-19 if the frequency is above twenty breaths per minute. The prototype algorithm was first tested on 12 sinusoidal code-generated signals. Using a threshold of 0.333 Hz (20 breaths per minute) as the minimum frequency indicative of COVID-19 breathing, the algorithm was able to classify the 12 different signals with 100% accuracy. The artificial sampling rate was 10 frames per second and 1200 samples were taken. Each signal was a combination of a pure sinusoid and random noise generated by the digital signal processing software.

IV. Results

Respiratory rate accuracy results for the robotic mover experiment are shown in Fig. 5. Despite the presence of significant noise, the results show that algorithm measured rates had an average frequency difference of about 0.0003 Hz compared to the programmed value, which is much better than the 0.01667-Hz value corresponding to 1 breath per minute accuracy.

The same algorithm was used in another experiment to measure human respiration, illustrated in Fig. 6. The wireless communications cards were set up in the same way as the robotic mover experiment. To be as close to the same frequencies as the robotic mover, the subject breathed with the help of a metronome. A piezoelectric chest belt was also used on the subject to attain a comparative measurement. The average difference between the frequency of the actual breathing and the extracted frequency across all 20 trials was 0.007650 Hz, which is less than 1 breath per minute (0.01667 Hz). The confidence interval, or range around the averages for

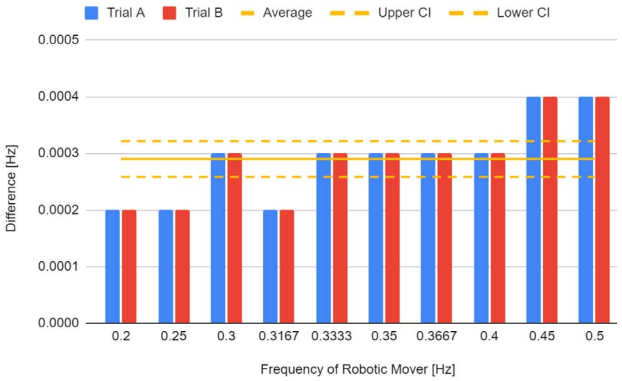

Fig. 5. Frequency difference for 20 robotic mover trials. All error was less than one breath/minute. The solid yellow line represents the average error, and the dashed yellow lines represent the 95% confidence interval.

which there is a 95% chance that the true value lies within, was +/- 0.003274. These results are summarized in Fig. 7.

This study was limited to measurements made with only a single sedentary subject within the field of view of the radar system. While the results represent a useful scenario, a system that can accommodate multiple subjects would be more robust. Physiological radar has been demonstrated to be effective in the presence of multiple subjects using various signal processing approaches including independent component analysis and blind source separation, which may be combined

Fig. 6. Experimental set-up for respiration measurement. Both Tx and Rx cards were about two meters away from the subject.

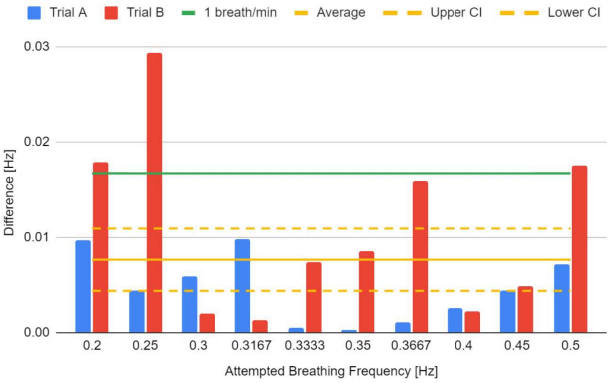

Fig. 7. Frequency difference in 20 respiration trials. Average error is less than one breath/minute. The solid yellow line represents the average error, and the dashed yellow lines represent the 95% confidence interval.

with the approach reported here to broaden scenarios of applicability [9,10].

V. Conclusion

The data supports that Doppler radar implemented with wireless communications cards can be used to create a COVID-19 screening mechanism that can be administered at a safe distance. The created algorithm differentiated between frequencies that only varied by 1 breath per minute, showing that it is sensitive to small changes that could be early indicators of a COVID-19 infection. The average frequency error was about 0.082%, much less than the 5% maximum stated in the engineering goal and lower than the typical error in medical settings. Measuring respiratory rate the traditional way, by counting breaths for 15 seconds, is not very accurate due to the small number of samples and potential for human error. The system created in the project provides an objective method, less subject to human error, for measuring respiratory rate. In addition, the system can leverage existing communication devices that most people already have within their own homes. This technology could serve as a practical, safe, and accurate COVID-19 screening device to help stop the spread and enable society to return to normal life.

Acknowledgment

The authors would like to thank all the members of the Wireless and Biosensing labs at the University of Hawaii Manoa who helped with these experiments.

References

[1] Harvard Health Publishing, "If you've been exposed to the coronavirus," *Harvard Health*, Sep. 24, 2020. https://www.health.harvard.edu/diseases-and-conditions/if-youve-been-exposed-to-the-coronavirus#:~:text=We%20know%20that%20a%20person (accessed Sep. 30, 2020).

[2] K. Schive, "I've been exposed to COVID-19; how soon will I be contagious? | MIT Medical," *medical.mit.edu*, Oct. 02, 2020. https://medical.mit.edu/covid-19-updates/2020/10/exposed-to-covid-19-how-soon-contagious.

[3] G. Shafiq and K. C. Veluvolu, "Surface Chest Motion Decomposition for Cardiovascular Monitoring," *Scientific Reports*, vol. 4, May 2014, doi: 10.1038/srep05093.

[4] S. B. Park and D. Khattar, "Tachypnea," *PubMed*, 2020. https://www.ncbi.nlm.nih.gov/books/NBK541062/#:~:text=Tachypnea%20in%20adults%20is%20breathing.

[5] Y. Wang, M. Hu, Q. Li, X.-P. Zhang, G. Zhai, and N. Yao, "Abnormal respiratory patterns classifier may contribute to large-scale screening of people infected with COVID-19 in an accurate and unobtrusive manner," *arXiv:2002.05534 [cs, eess]*, Dec. 2020, Accessed: Feb. 17, 2021. [Online]. Available: https://arxiv.org/abs/2002.05534.

[6] D. J. Miller *et al.*, "Analyzing changes in respiratory rate to predict the risk of COVID-19 infection," *PLOS ONE*, vol. 15, no. 12, p. e0243693, Dec. 2020, doi: 10.1371/journal.pone.0243693.

[7] C. Li, V. M. Lubecke, O. Boric-Lubecke, and J. Lin, "A Review on Recent Advances in Doppler Radar Sensors for Noncontact Healthcare Monitoring," *IEEE Transactions on Microwave Theory and Techniques*, vol. 61, no. 5, pp. 2046–2060, May 2013, doi: 10.1109/tmtt.2013.2256924.

[8] X. Wang, C. Yang, and S. Mao, "Resilient Respiration Rate Monitoring With Realtime Bimodal CSI Data," *IEEE Sensors Journal*, vol. 20, no. 17, pp. 10187–10198, Sep. 2020, doi: 10.1109/JSEN.2020.2989780.

[9] S. M. M. Islam, E. Yavari, A. Rahman, V. M. Lubecke and O. Boric-Lubecke, "Separation of Respiratory Signatures for Multiple Subjects Using Independent Component Analysis with the JADE Algorithm," *2018 40th Annual International Conference of the IEEE Engineering in Medicine and Biology Society (EMBC)*, 2018, pp. 1234-1237, doi: 10.1109/EMBC.2018.8512583.

[10] Olga Boric-Lubecke; Victor M. Lubecke; Amy D. Droitcour; Byung-Kwon Park; Aditya Singh, "Applications and Future Research," in Doppler Radar Physiological Sensing, IEEE, 2016, pp.269-284, doi: 10.1002/9781119078418.ch9.